Appropriate Switched Reluctance Generator for Wind Energy Domestic: Design and Electromagnetic Performance

IMED MAHMOUD[1,3,*], ADEL KHEDHER[2,3]
[1]University of Monastir,
Higher Institute of Applied Science and Technology of Mahdia,
Street Rejiche 5121 Mahdia,
TUNISIA

[2]University of Sousse,
National Engineering School of Sousse,
BP 264 Sousse Erriadh 4023,
TUNISIA

[3]Laboratory of Advanced Technology and Intelligent Systems (LATIS),
National School of Engineers of Sousse,
BP 264 Sousse Erriadh 4023
TUNISIA

**Corresponding Author*

Abstract: - This study explores the suitability of Switched Reluctance generators (SRGs) for domestic wind energy applications, focusing on design considerations and electromagnetic performance factors. The design aspects encompass rotor and stator configurations, integration with wind turbines, and material selection for durability and cost-effectiveness. Electromagnetic performance factors such as torque density, efficiency, power factor, and control system integration are crucial for optimizing energy conversion and system stability. Our goal is to enhance torque performance by carefully selecting the number of phases and varying combinations of stator and rotor pole numbers (specifically, 6/4, 8/6, and 12/8). To ensure a fair comparison, we maintain the same main dimensions across all topologies. This involves key parameters such as the inner and outer diameters of the stator, the height of the rotor poles, the air gap length, the stator pole height, the stack length, and the width of the stator yoke. Our analysis has revealed that increasing the extinction angle has a significant impact on the system's behavior. These observations highlight the intricate nature of the system's dynamics and stress the need for careful optimization of these parameters to achieve superior performance. By addressing these factors, SRGs can serve as a dependable and efficient solution for producing wind energy in residential areas, thereby promoting Greater access to renewable and sustainable energy sources for households.

Key-Words: - Switched Reluctance generator, different topology, Torque, renewable energy, FEA, extinction angle and residential energy.

Received: June 20, 2024. Revised: March 2, 2025. Accepted: April 1, 2025. Published: May 12, 2025.

1 Introduction

Renewable energies (wind, solar, geothermal, etc.) offer an alternative that ensures pollution-free production, no greenhouse gas emissions, and low costs. These advantages have made wind energy, in particular, one of the most competitive energy sources. The efficiency of wind turbines primarily depends on the performance and output of the integrated electric generator, the effectiveness of the implemented control system, and the power converter that connects it to the grid. Currently, two types of generators dominate this category of wind turbines: the permanent magnet synchronous machine, known for its high efficiency, and the doubly-fed induction generator, appreciated for its relatively simple electromagnetic design. However, both remain relatively expensive and challenging to manufacture. Still, other types of generators are currently under development.

To reduce costs and improve the autonomy of Wind Energy Conversion Systems, manufacturers have explored a competitive solution through the Switched Reluctance Generators (SRG). This generator offers control flexibility, a wide speed range without the need for a gearbox, which is often the source of frequent breakdowns and requires periodic preventive maintenance, and high power density, [1], [2], [3], [4], [5]. Nevertheless, a notable drawback of SRGs lies in the dependency of phase inductance on both current and rotor positions in the active phase, presenting challenges in modeling, control, and characterization. To address these hurdles, the finite element method (FEM) is commonly utilized as a pivotal tool for comprehending various critical aspects in the design and effective implementation of SRGs. Operating in motor and generator modes, SRMs exhibit increased appeal in applications requiring variable speed operations, whether as a motor or generator. SRMs find extensive applications across a spectrum of domains, including domestic appliances, compressors, turbochargers, wind power generation, electric vehicles, and oil pumps, among others, [6], [7], [8], [9].

The design process for SRMs necessitates a multidisciplinary approach encompassing considerations such as acoustic, thermal, mechanical, and electromagnetic aspects. In industrial applications, cost and technological factors hold significant weight in decision-making. The design process strives to identify the optimal combination of topology, geometry, and materials that align with specific application requirements like weight, size, fault tolerance, and minimal torque ripple, [10], [11], [12], [13], [14]. The selection of the appropriate topology for a given application stands out as a complex challenge during the design phase. While implementing an optimization design procedure for topology selection remains challenging, experience-based methods persist as the most frequently employed approach. Design optimization efforts aimed at enhancing SRG performance have sparked interest, [15], [16], [17], [18].

This paper delves into comparative investigations among doubly salient synchronous reluctance machines stemming from the aforementioned SRMs, encompassing three distinct topologies and winding configurations, as depicted in Figure 1. Different numbers of phases and different combinations of rotor and stator pole numbers will be considered, keeping the same main dimensions (outer and inner stator diameter, stator pole height, air gap length, stator yoke width, rotor pole height stack length) and the same winding per phase (wire diameter and number of turns).

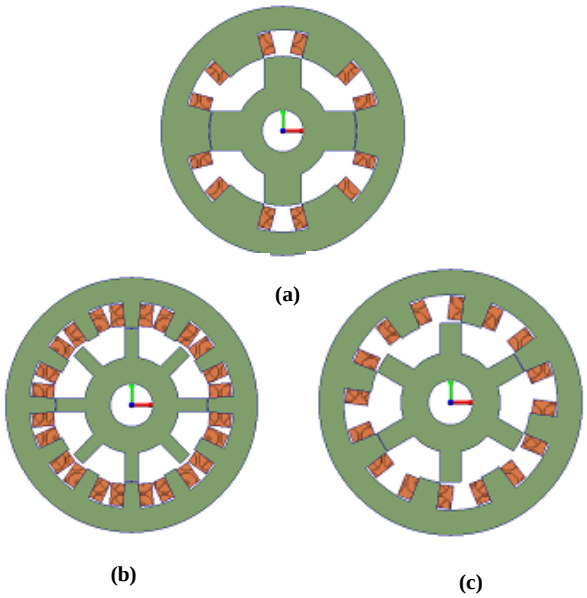

Fig. 1: SRG topology

A preliminary sizing of the machine will be taken on, giving the initial geometric, [19]. The key dimensions will be calculated and the winding will be dimensioned. The phase winding of the machine is energized by a rotor fixed to a certain position by a stepping motor and with a pulsed DC voltage. Then the flux-linkage characteristics are indirectly calculated based on the phase current, voltage, and resistance. The torque characteristics are obtained directly by the static torque transducer. A numerical-based performance analysis (flux-linkage, static torque characteristics...) will be performed for each case to provide a preliminary evaluation of their suitability for meeting the stringent requirements of embedded machines in aerospace applications. The comparison of the results will give a good solution for the SRM topology.

2 Preliminary Sizing of SRG

The preliminary sizing process involves selecting the optimal number of phases and determining the stator and rotor pole numbers. Additionally, the dimensions of the stator and rotor, such as their diameters, pole heights, and stack length, are established. These parameters are crucial in achieving the desired performance characteristics and ensuring the proper operation of the SRG, [20].

The choice of a number of stator poles *Ns* and a number of rotor poles *Nr* is important since they

have significant implications on the torque. Usually, *Ns* is selected greater than *Nr* with the following relation: Least-Common-Multiple (Ns, Nr) = qNr. The speed is related to the frequency of the power supply according to the mode of supply (f=Nr.N/m). With unidirectional (m=1) or alternative (m=2).

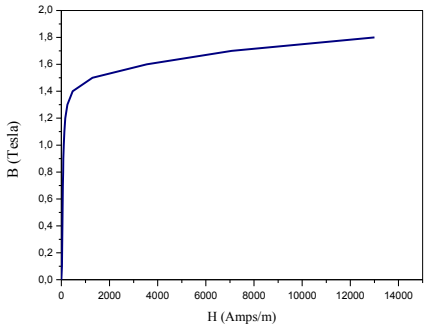

Fig. 2: Magnetic curve of sheets of iron N020

We used a ferromagnetic material N020 with ε=0.20mm thickness for the different structures SRGs (Figure 2), due a magnetic, thermal, mechanical properties and manufacturing cost. The B-H characteristics of this material, which will be used in the stator and rotor stampings, have to be examined, Figure 2. Figure 3 illustrates all the dimensions that must be determined for the construction of an SRG, where *g* is the length of the air gap, *Ds* is the outer diameter, *Dr* is the inner diameter, D_0 is the shaft diameter, βr is the rotor pole arc, βs is the stator pole arc, *Hs* is the stator pole height, *Hr* is the rotor pole height, *Ys* is the stator back iron thickness, and *Yr* is the rotor back iron thickness.

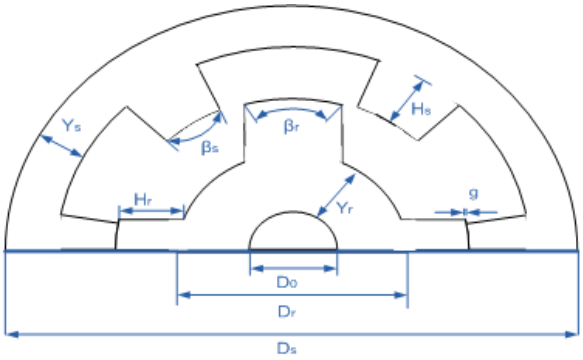

Fig. 3: Diagram of the SRG

The important factor in motor design optimization, torque ripple, duration of output torque, and winding space is the choice of βs and βr. We choose the angles of two teeth through the three following conditions, [21], [22], [23]:

$$\beta sm = \left(\frac{2\pi}{qNr}\right) = 30° \le \beta s \le 45° = (\pi / Nr) \quad (1)$$

$$\beta rm = \beta sm = 30° \le \beta r \le 60° = (a_r - \beta sm) \quad (2)$$

$$(\beta s + \beta r) < a_r = \left(\frac{2\pi}{Nr}\right) = 90° \quad (3)$$

The machine dimensions and their impact on performance are characterized by implicit relationships and made available in a form to enable machine design. Further, the standard design procedure begins with the power output equation relating to the machine dimensions. The output power for an electrical machine is proportional to the product of specific electric and magnetic loadings, air gap diameter, and effective stack length, [24].

The estimations prompting the selection of the conductor and the winding design are as per the following. Expecting a wedge of H_{wedge} is required to hold the windings in place, the stator slot arc length L_s at the closest point of the winding to the center of the shaft is given by:

$$L_s = \left(\frac{D}{2} + H_{wedge}\right)\beta_S \quad (4)$$

The minimum area of conductor A_S assuming a maximum value of allowable current density J in the windings is given by [25],

$$A_s = \frac{i_t}{J} \quad (5)$$

Presently a standard size conductor is picked in light of the estimation of as_s computed previously. The wire diameter D_{wire} including insulation is given by [25]

$$D_{wire} = 2.\sqrt{\frac{A_S}{\pi}} + 0.1mm \quad (6)$$

Representing the wedges that hold the windings in place leads to the calculation of a modified stator pole pitch λ as,

$$\lambda = \frac{\pi}{Ns}\left(2R_r + 2h_{wedge}\right) = L_s + S \quad (7)$$

The maximum height of the winding H_{wedge} which can be accommodated inclusive of the space required to place wedges that hold the windings in place is given by

$$H_w = H_s - H_{wedge} \quad (8)$$

Two important aspects to be considered in the SRM design are the number of vertical and horizontal layers, [25].

The number of vertical layers that can be suited to this available winding height is given by:

$$n_V = \frac{H_w.F_f}{D_{wire}} \quad (9)$$

With F_f represents the field factor and is approximately equal to 0.95. The value of n_v is rounded off to the nearest lower integer. And the number of horizontal layers n_H required for winding is given by:

$$n_H = \frac{N_t}{2.N_c} \quad (10)$$

The value of n_H is rounded off to the nearest higher integer. It is desirable that the width of the rotor and stator pole should be equal or almost equal. The optimum pole widths must be chosen considering the maximization of the aligned phase inductance, high inductance ratio, and mechanical stiffness. Presently, the width of the winding for stator W_L is given by:

$$W_L = \frac{D_{wire}.n_H}{F_f} \quad (11)$$

In order to determine the winding size, it is necessary to obtain an available winding area in the interval of two stator poles and a clearance C between the two adjacent coils (Figure 3). The maximum stator coil area for a rectangular shape is:

$$C = L_s - (2W_L) \quad (12)$$

The machine parameters are assembled in Table 1.

Table 1. Motors mechanical parameters

Parameters	unit	8/6 SRM	12/8 SRM	6/4 SRM
Rotor pole angle	βr	24.5°	17°	32°
Stator pole angle	βs	22.5°	15°	30°
Stator external	Ds	160mm	160mm	160mm
diameter	Dr	91.1mm	91.1mm	91.1mm
Rotor diameter	g	0.3mm	0.3mm	0.3mm
Air gap length	Hr	13mm	13mm	13mm
Stator pole height	Hs	22mm	22mm	22mm
Rotor pole height	Ys	12.45mm	12.45mm	12.45mm
Rotor yoke	Yr	15mm	15mm	15mm
Stator yoke	D0	34.5mm	34.5mm	34.5mm
Shaft diameter				

2 Electromagnetic Performances of SRG

Motor design is subjected to FE-based magnetic field analysis, and torque ripple is suppressed by providing teeth on the stator/rotor poles [26], The FE method is a powerful electromagnetic simulation technique based on numerical analysis. The phases in SRG are identical to each other, so only one phase is selected for measurements from an aligned position to an unaligned position, and the characteristics of other phases can be obtained with appropriate phase shifts. The initial rotor position is the aligned position, which can be easily found by energizing one phase.

To understand the electromagnetic characteristics of a switched reluctance generator (SRG), it is essential to conduct an in-depth analysis of field lines, meshing techniques, magnetic field distribution, and induction vectors. These evaluations are fundamental for understanding the behavior and performance of SRGs, thereby enabling improvements in design and optimization of overall efficiency.

Magnetic field lines clearly illustrate the magnetic flux patterns within an SRG, facilitating the analysis of the field's direction, strength, and distribution. By carefully examining these field lines, Figure 4, Figure 6 and Figure 8, it is possible to identify areas with variable flux intensity, which influence torque generation and the overall efficiency of the system. This understanding forms the foundation for optimizing geometric structures, winding configurations, and control strategies, contributing to enhanced performance.

Analyzing meshed designs makes it possible to identify issues such as magnetic saturation, flux leakage, and excessive losses, Figure 4, Figure 6 and Figure 8. This detailed feedback supports design improvements, ensuring better performance, efficiency, and reliability. A thorough investigation of the magnetic field distribution also provides critical insights into flux density, flux coupling, and the forces acting within the machine. Detecting flux imbalances or saturation zones allows for specific design adjustments to minimize losses and improve both torque efficiency and operational effectiveness.

Electromagnetic induction, represented by induction vectors, also plays a key role in evaluating SRGs, Figure 5, Figure 7 and Figure 9. These vectors highlight the interactions between the stator and rotor poles, which directly influence the torque and efficiency of the machine.

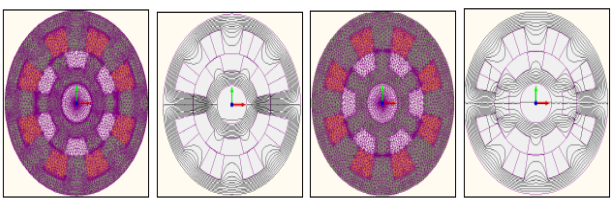

Fig. 4: Configuration of magnetic flux lines and mesh concentration at the two extreme positions for SRG 8/6

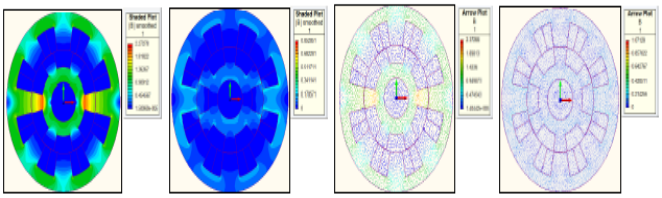

Fig. 5: Variation of the magnetic field and induction vector at the two outer positions for SRG 8/6

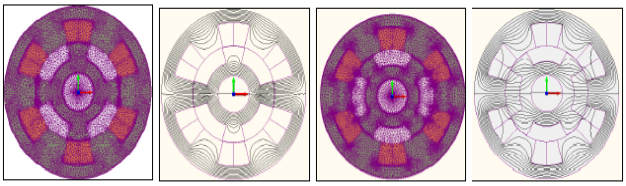

Fig. 6: Configuration of magnetic flux lines and mesh concentration at the two extreme positions for SRG 6/4

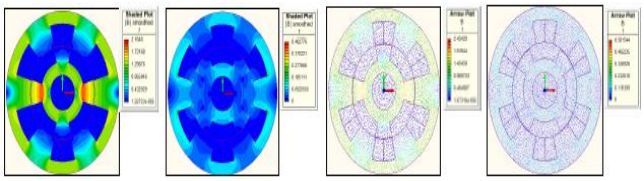

Fig. 7: Variation of the magnetic field and induction vector at the two outer positions for SRG 6/4

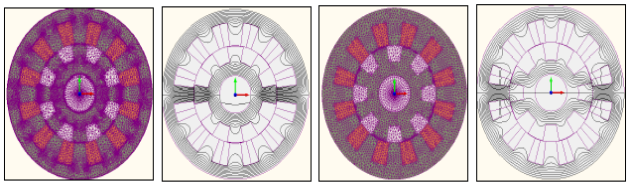

Fig. 8: Configuration of magnetic flux lines and mesh concentration at the two extreme positions for SRG 12/8

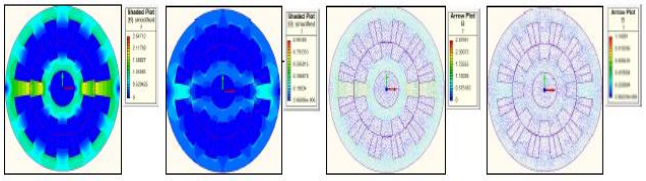

Fig. 9: Variation of the magnetic field and induction vector at the two outer positions for SRG 12/8

Finite Element analysis has been used to investigate the behavior of the SRG over a range of 25 phase current values, covering three different SRG configurations.

The maximum current analyzed is set at 25A, with increments of 1A. The results are shown in the accompanying figures.

- Figure 10 shows the FE results showing the linkage flux for varying phase currents and rotor positions in SRG configurations of 6/4, 8/6, and 12/8. Figure 10(a): The flux linkage patterns for the 6/4 SRG design (six stator poles and four rotor poles) are shown, illustrating how the flux behavior changes with phase current and rotor position.
- Figure 10(b): The results for the 8/6 SRG configuration highlight the relationship between linkage flux and phase currents, showing how the electromagnetic characteristics change with changes in rotor position. This design has eight stator poles and six rotor poles.
- Figure 10(c): For the 12/8 SRG design (twelve stator poles and eight rotor poles), the flux linkage trends are plotted, showing how variations in phase current affect the magnetic flux at different rotor positions.

The maximum phase current analyzed for these three configurations is set at 25A, with measurements taken at mechanical angle increments of 2.5°. These findings are crucial for understanding and optimizing the electromagnetic behavior of SRGs.

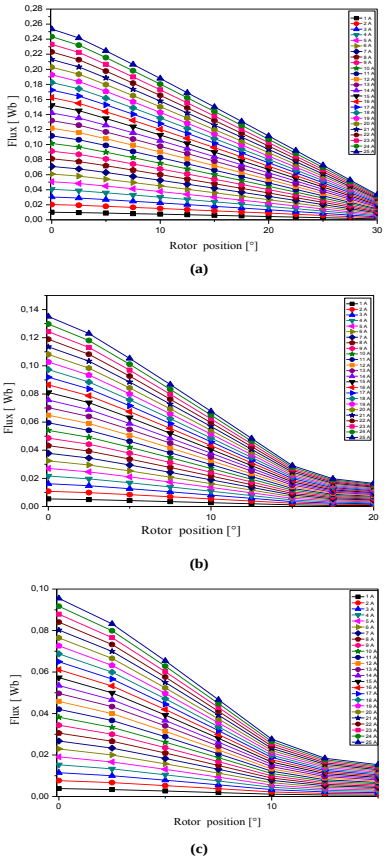

Fig. 10: FE results of linkage flux versus phase currents for different rotor positions:
a) SRG 6/4, b) SRG 8/6 and c) SRG 12/8.

Figure 11 presents the finite element (FE) results depicting the torque as a function of rotor positions and different current values for three different types of SRG 6/4, SRG 8/6, and SRG 12/8.

For domestic energy applications, the choice of SRG topology should consider the following criteria:

- **Torque Requirements**: If high starting torque and efficiency are crucial, a higher pole count like 12/8 may be suitable.
- **Energy Efficiency**: Higher pole count configurations often offer better efficiency but come at a higher cost.
- **Cost Considerations**: If cost is a significant factor, the 6/4 or 8/6 configurations might be more appropriate.
- **Application Complexity**: A simpler configuration like 6/4 may be easier to control and maintain for domestic usage.

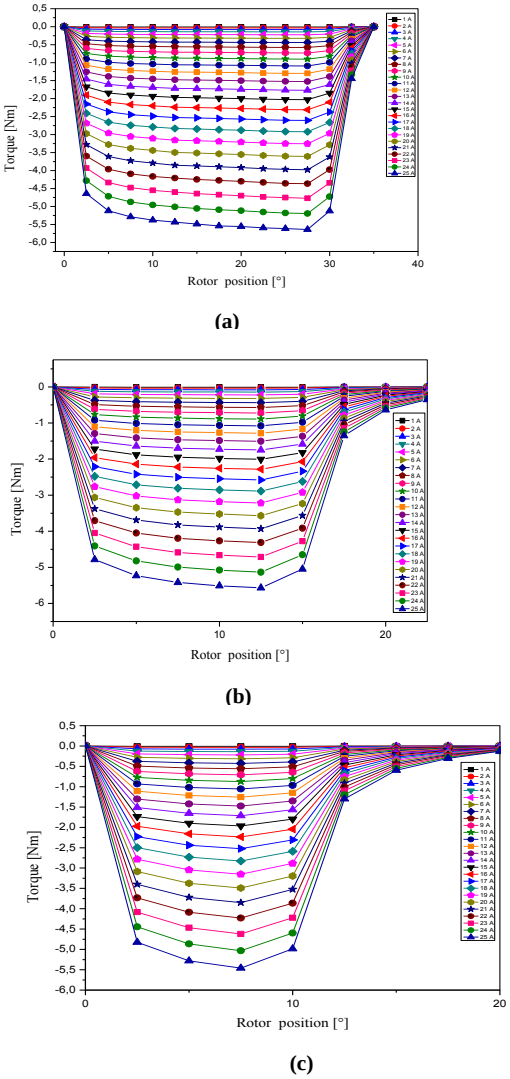

Fig. 11: FE results of torque versus positions and different current values
a) SRG 6/4, b) SRG 8/6 and c) SRG 12/8.

Based on these criteria, for domestic energy applications where cost is a significant factor and moderate torque requirements are needed, the 6/4 SRG topology might be the most suitable choice. It strikes a balance between cost-effectiveness and performance, making it a practical option for domestic energy systems.

3 Mathematical Model and Operation modes of SRG

The main assumption for the study (machine-converter) is a total decoupling of the phases: no magnetic coupling (no mutual) or electrical coupling (no electrical connection between windings of two different phases). A switched reluctance machine is a double salient machine. It operates as a generator if each phase is excited when the phase inductance decreases, as shown in Figure 12. The SRG phase-k voltage u_k can be expressed as Equations (13), (14) and (15). Where i_k is the phase-k current, r is the windings resistance, θ is the rotor position, $L_k(\theta, i_k)$ is the phase inductance, $\varphi_k(\theta, i_k)$ is the flux-linkage, ω is the rotor angular velocity, and e_k represents the back-emf, [24], [25], [26], [27]:

$$u_k = r\, i_k + \frac{d\varphi_k(\theta, i_k)}{dt},\ k = (1,2,3) \tag{13}$$

$$u_k = r\, i_k + L_k(\theta, i_k)\frac{di_k}{dt} + e_k,\ k = (1,2,3) \tag{14}$$

With

$$e_k = i_k \frac{d\theta}{dt}\frac{dL_k(\theta, i_k)}{d\theta},\quad \frac{d\theta}{dt} = \omega \tag{15}$$

The mechanical behavior of the SRG is described by Equation 16.

$$J\frac{d\omega}{dt} = T_e(\theta, i_1, i_2, i_3) - T_L - f\,\omega \tag{16}$$

Where J is the inertia of the machine, f is the friction coefficient, and T_L is the load torque. $T_e(\theta, i_1, i_2, i_3)$ is the global electromagnetic torque of the machine.

Under the assumptions of no magnetic saturation and no mutual coupling between the phases, the elementary torque can be expressed as:

$$T_e(\theta, i_k) = \frac{1}{2} i_k^2 \frac{dL_k(\theta, i_k)}{d\theta} \tag{17}$$

We can see from Equation 17 that SRG torque production depends on the current amplitude and inductance variation with the rotor position. This

equation also shows that the torque sign only depends on the inductance slope. Therefore, to produce a negative torque, the phase winding should be excited when the inductance decreases. Figure 12 shows the relationship between the phase inductance and rotor position.

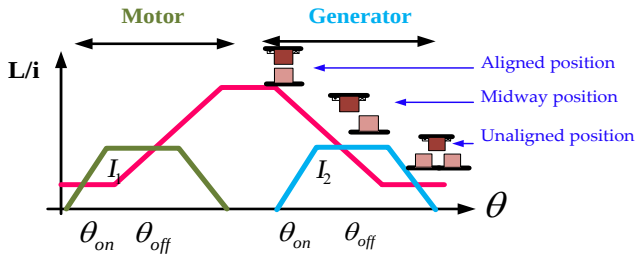

Fig. 12: Inductance and current variation versus rotor position

Many converter topologies can be used to ensure the operation of SRG, Figure 13. One such converter is the asymmetric half-bridge converter (AHBC). The AHB converter is widely used due to its robustness and simplicity of control. It provides unidirectional phase currents and operates each phase independently. The AHB converter consists of two transistors and two freewheeling diodes in each phase.

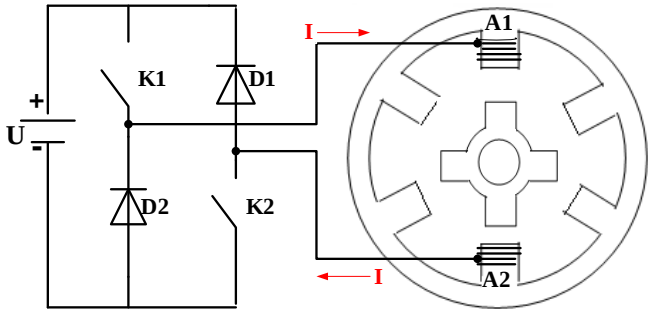

Fig. 13: Power supply of an SRG phase

In order to operate as a generator, the required steps to activate the AHBC are shown in Figure 14. In the excitation step, Figure 14(a), both switches S_1 and S_2 are activated and the excitation voltage DC is supplied. In the generation step, Figure 14(b), S_1 and S_2 are both turned off and the electric current flows through the diodes D_1 and D_2 through the SRG winding and then back to the DC source. Finally, when S_1 is deactivated, the current flows through the diode D_2 in freewheel mode. In this stage, the voltage is zero and there is no power flow between the machine and the source, Figure 14(c).

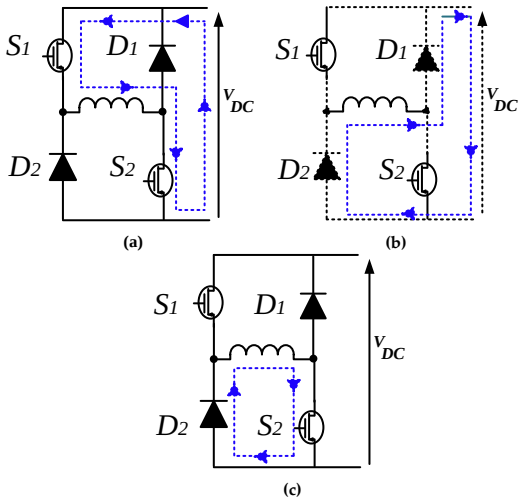

Fig. 14: AHBC connected to SRG
(a)- Excitation stage (b)- Generation stage (c)- Freewheeling stage

4 Effect of Varying the Extinction Angle on SRG Dynamic Performance

Figure 15 shows the Simulink model of the SRG. This model consists of the block GRVDS, power converter, power and position sensor block, and current hysteresis controller). The scope is used to view the variation of main parameters.

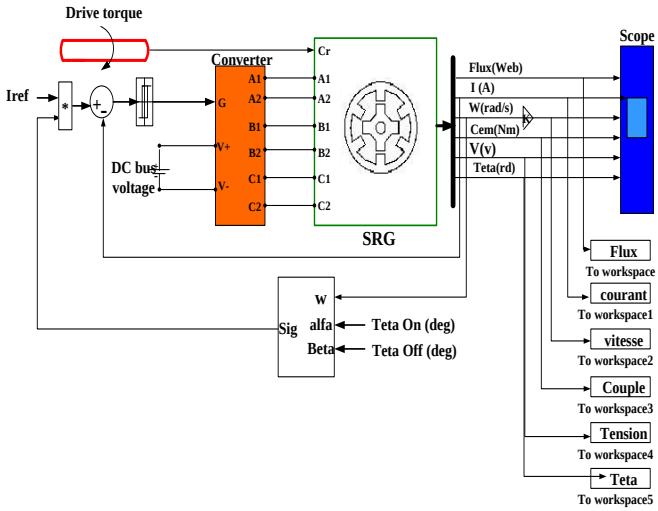

Fig. 15: Bloc diagram of SRG 6/4

The SRG will be driven by a load torque of 100Nm at a DC bus voltage of 230 V, to magnetize the generator, Θ_{on}=74° and Θ_{off} =[20° and 28°]. Figure 16 show the simulation results.

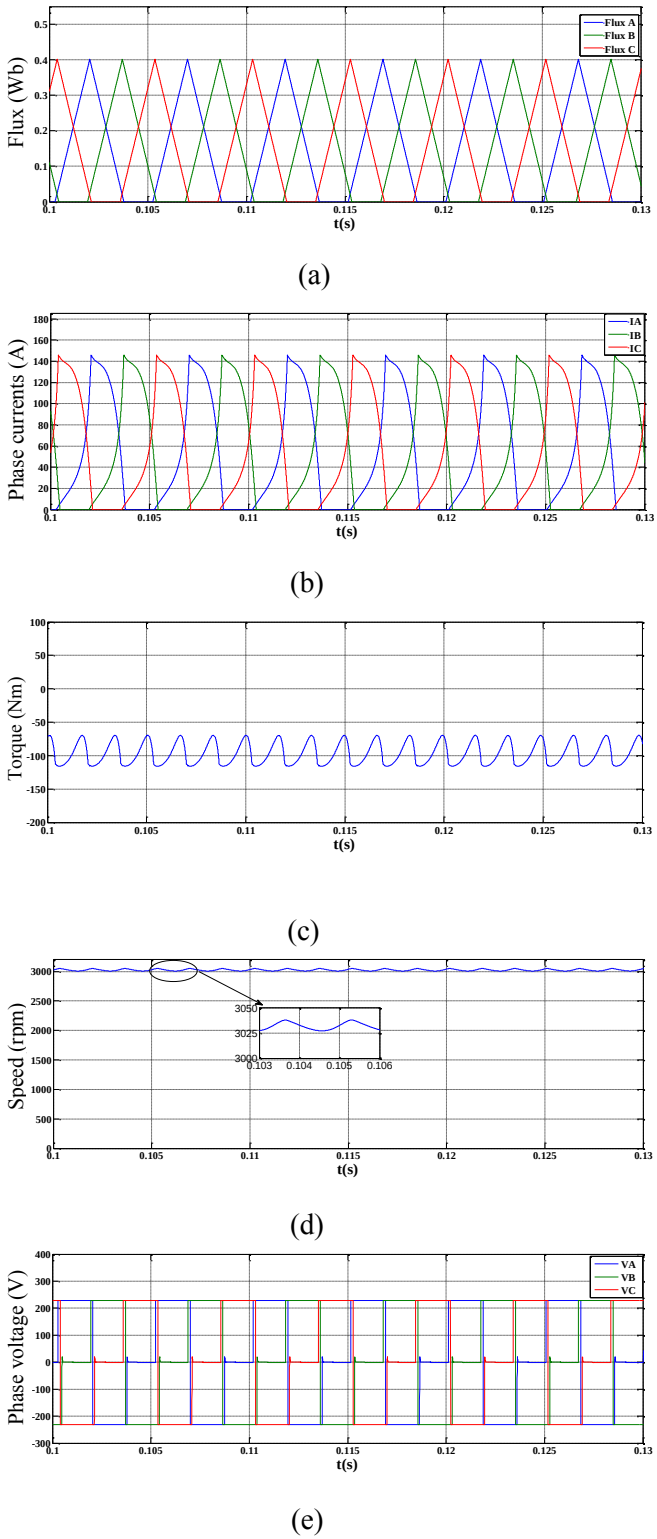

Fig. 16: SRG dynamic performance, Θ_{on}=74° and Θ_{off} =20°

In our investigation, the impact of increasing the angle of extinction on the system dynamics has been notably observed, Figure 17. As the angle of extinction is augmented, a discernible decrease in speed is noted, indicating a direct relationship between this parameter and the rotational velocity of the system. This reduction in speed correlates with a convergence of the average torque towards the load torque value, signaling a shift in the balance of forces within the system.

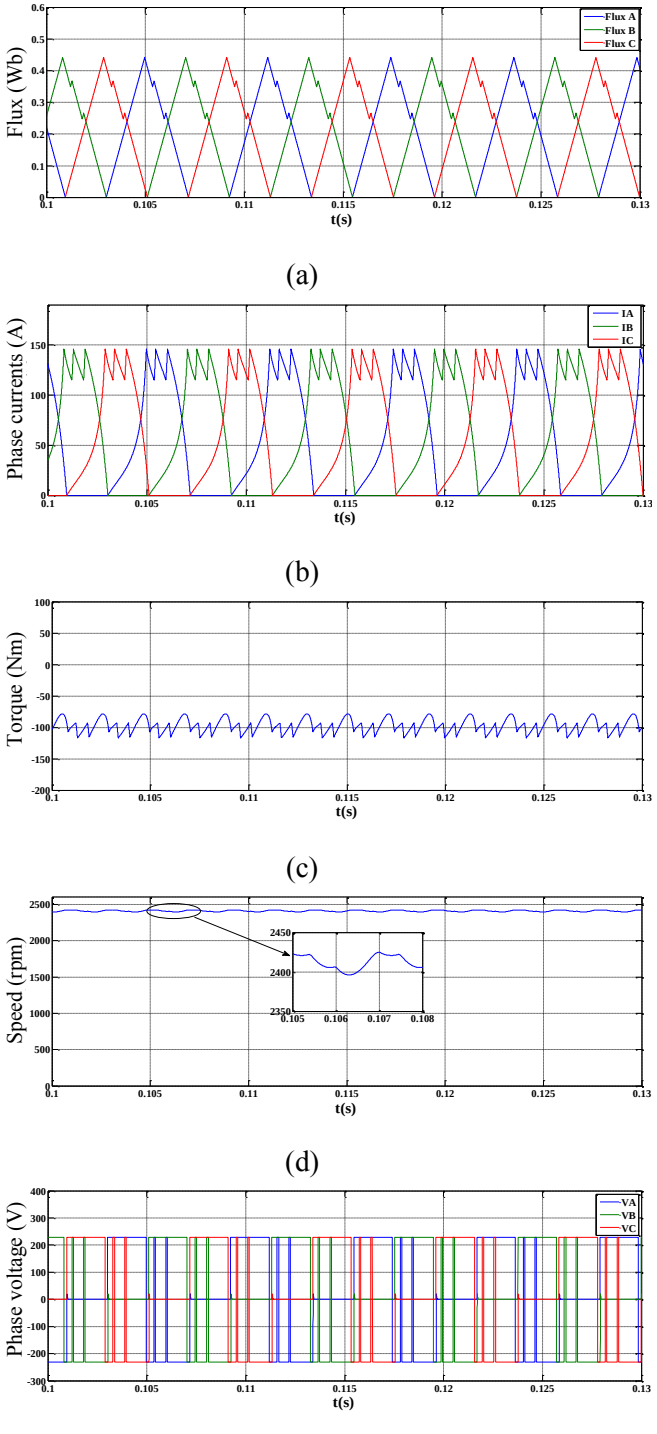

Fig. 17: SRG dynamic performance, Θ_{on}=74° and Θ_{off} =28°

Moreover, the system exhibits more pronounced oscillations as the extinction angle increases, indicating an enhanced responsiveness to variations

in operating conditions. Simultaneously, a slight but noticeable increase in the average current is observed, reflecting a minimal rise in the electrical load on the system components. This correlation between the extinction angle and system performance highlights the complex interactions among operational parameters and the system's behavior in various contexts. These observations provide insight into the complex dynamics of the system and underscore the importance of adjusting parameters to achieve the desired performance.

5 Conclusion

Wind energy is currently one of the most exploited renewable sources, given its feasibility for conversion compared to other sources. However, experimenting with new topologies and control strategies for wind energy conversion systems poses certain challenges that slow down the development in this field. Electric machines play a significant role in industrial energy consumption. It is therefore essential to enhance their efficiency and reliability by developing new high-performance control laws. After conducting a thorough analysis of switched reluctance generators (SRGs) within the realm of residential wind turbines, valuable insights have been gleaned regarding crucial design elements and electromagnetic performance standards. This exploration is pivotal for enhancing energy conversion efficiency and ensuring system stability. Various configurations such as 6/4, 8/6, and 12/8 have been scrutinized while maintaining consistent primary dimensions to establish a reliable foundation for comparison. This approach has enabled a comprehensive examination of system behavior, encompassing the impact of adjusting the turn-off angle.

While the 6/4 model boasts a simplistic design, cost-effectiveness, and robust performance, it does exhibit nonlinear electromagnetic characteristics and a diminished power factor. Nonetheless, it remains a formidable contender against conventional machines.

The findings underscore the intricate dynamics of SRG systems and underscore the importance of parameter optimization for achieving peak performance. This underscores the reliability and efficiency of switched reluctance machines (SRMs) as a viable solution for residential wind power generation, effectively meeting the escalating demand for sustainable and cost-effective renewable energy solutions in households. This study sets the stage for future progressions, paving the way for the advancement of more sophisticated and efficient approaches to harnessing wind energy in domestic settings.

Declaration of Generative AI and AI-assisted Technologies in the Writing Process:

The authors wrote, reviewed and edited the content as needed and have not utilised artificial intelligence (AI) tools. The authors take full responsibility for the content of the publication.

References:

[1] T. Miller: “Switched reluctance motors and their control” Hillsboro, OH: Magna Physics; Oxford: Clarendon Press; New York: Oxford University Press, Monographs in electrical and electronic engineering; 31, ISBN: 1881855023, OCLC: 1013387969, (1993)

[2] R. Krishnan, “Switched Reluctance Motor Drives: Modeling, Simulation, Analysis, Design, and Applications” Boca Rsaton, FL, USA: CRC Press (2001), https://doi.org/10.1201/9781420041644.

[3] S. Sezen, E. Karakas, K. Yilmaz, and M. Ayaz, “Finite element modeling and control of a high-power SRM for hybrid electric vehicle” *Simul. Model. Pract. Theory.*, Vol.62, pp.49-67 (2016), https://doi.org/10.1016/j.simpat.2016.01.006.

[4] A.L.M. Santos, J. Anthonis, F. Naclerio, J.J.C. Gyselinck, H. V. d. Auweraer and L.C.S. Goes, “Multiphysics NVH modeling: simulation of a switched reluctance motor for an electric vehicle” *IEEE Trans. Ind. Electron.*, Vol.61, pp.469-476 (2014), https://doi.org/10.1109/TIE.2013.2247012.

[5] I. Mahmoud and A. Khedher, “Artificial neural network-based control of a switched reluctance motor for a high-precision positioning system”, *Engineering World*, Volume 6, (2024), https://doi.org/10.37394/232025.2024.6.14.

[6] M. Takeno, N. Hoshi, A. Chiba, M. Takemoto, and S. Ogasawara, “A comparison of high power and high efficiency machines of 50 kW SRM designed for HEVs,” (in Japanese), *in Proc. Annu. Conf. IEEJ Ind. Appl. Soc.*, Vol. 3, pp. 407–412 (2011).

[7] S. Inamura, K. Sawa, “A Study on Temperature Analysis of Switched Reluctance Motor,” *IEEJ Trans. IA*, Vol.123, pp.422-428 (2003), https://doi.org/10.1541/ieejias.123.422.

[8] C. Sahin, A. E. Amac, M. Karacor, and A. Emadi, "Reducing torque ripple of switched reluctance machines by relocation of rotor moulding clinches" *IET Elec. Power Appl.,* Vol.6, pp.753-760 (2012), https://doi.org/10.1049/iet-epa.2011.0397.

[9] T.J.E. Miller, "Optimal design of switched reluctance motors" *IEEE Trans. Ind. Electron.,* Vol.49, pp.15-27 (2002), https://doi.org/10.1109/41.982244.

[10] K. Kiyota and A. Chiba, "Design of Switched Reluctance Motor Competitive to 60-kW IPMSM in Third-Generation Hybrid Electric Vehicle" *IEEE Trans. Ind. Appl.,* Vol.48, pp.2303-2309 (2012), https://doi.org/10.1109/TIA.2012.2227091.

[11] J. D. Widmer, R. Martin, and B. C. Mecrow, "Optimization of an 80-kWSegmental Rotor Switched Reluctance Machine for Automotive Traction" *IEEE Trans. Ind. Appl.,* Vol.51, pp.2990-2999 (2015), https://doi.org/10.1109/TIA.2015.2405051.

[12] K. Kiyota, T. Kakishima, and A. Chiba, "Comparison of test result and design stage prediction of switched reluctance motor competitive with 60-kW rare-Earth PM motor" *IEEE Trans. Ind. Electron.,* Vol.61,pp.5712_5721 (2014), https://doi.org/10.1109/TIE.2014.2304705.

[13] Z. Touati, I Mahmoud, R. E. Araújo, A. Khedher," Fuzzy Super-Twisting Sliding Mode Controller for Switched Reluctance Wind Power Generator in Low-Voltage DC-microgrid Applications", *Energies* (2024), 17, 1416, https://doi.org/10.3390/en17061416.

[14] J.B. Bartolo, and M. Degano, "Design and Initial Testing of a High Speed 45 kW Switched Reluctance Drive for Aerospace Application", *IEEE Transactions on Sustainable Energy*, Vol 64, pp.988 _ 997 (2016), https://doi.org/10.1109/TIE.2016.2618342.

[15] H. Chen and J. J. Gu, "Implementation of the three-phase switched reluctance machine system for motors and generators" *Trans.Mechatronics*, Vol.15, pp.421_432 (2010), https://doi.org/10.1109/TMECH.2009.2027901.

[16] Y. Hu, X. Song, W. Cao, and B. Ji, "New SR drive with integrated charging capacity for plug-in hybrid electric vehicles (PHEVs)" *Ind.Electron.,* Vol.61, pp.5722_5731 (2014), https://doi.org/10.1109/TIE.2014.2304699.

[17] C. Capovilla, I. Santana, A. Filho, T. Barros, and E. Ruppert, "Performance of a direct power control system using coded wireless OFDM power reference transmissions for switched reluctance aerogenerators in a smartgrid scenario" *Ind. Electron.*, Vol.62, pp.52_61 (2015), https://doi.org/10.1109/TIE.2014.2331017.

[18] T.A.S. Barros and E. R. Filho, "Direct power control for switched reluctance. Generator in wind energy" *IEEE Latin America Trans*., Vol.13, pp.123_128 (2015), https://doi.org/10.1109/TLA.2015.7040638.

[19] J. Almeida and A. Costa. "Design and Performance Evaluation of a Switched Reluctance Generator for Small-Scale Wind Turbines." *Journal of Energy Storage*, 45, 103170, (2022).

[20] L. Cheng and Q. Zhang. "Dynamic Modeling and Control of Switched Reluctance Generators for Wind Energy Systems." *IET Renewable Power Generation*, 17(4), 585-599, (2023).

[21] P.J. Lawrenson, J.M. Stephenson, P.T. Blenkinsop, J. Corda, N.N. Fulton, "Variable-speed switched reluctance motors", Proc. IEE. Electric Power Applications, Vol.127, pp.253-265 (1980), https://doi.org/10.1049/ip-b.1980.0034.

[22] B. Multon, "Pole Arcs Optimization of Vernier Reluctance Motors Supplied with Square Wave Current", *Elect. Mach. Power Syst*, vol.21, pp.695-709 (1993), https://doi.org/10.1080/07313569308909694.

[23] H. Liu, Y. Zhang and Wang. "Design and Optimization of a Switched Reluctance Generator for Wind Energy Applications." *Energy Reports*, 7, 123-135, (2021).

[24] S. Kumar and R.Gupta. "Performance Analysis of Switched Reluctance Generators for Small Wind Turbines." *Renewable Energy*, 186, 123-134, (2022).

[25] J. Zhou, Y. Li and Q. Chen. "Advancements in Switched Reluctance Generator Technology for Wind Energy Conversion Systems." *Journal of Renewable and Sustainable Energy*, 15(3), 456-472, (2023).

[26] A. Nadja and A. Salih. "Analysis of Electromagnetic Performance of Switched Reluctance Generators for Wind Energy Harvesting." *IEEE Transactions on Energy Conversion*, 35(2), 555-563, (2020).

[27] J. Fernandez and J. Moreno. "Control Strategies for Switched Reluctance Generators in Wind Energy Applications." *Energy Conversion and Management*, 257, 115-125, (2022).

Contribution of Individual Authors to the Creation of a Scientific Article (Ghostwriting Policy)

The authors equally contributed in the present research, at all stages from the formulation of the problem to the final findings and solution.

Sources of Funding for Research Presented in a Scientific Article or Scientific Article Itself

No funding was received for conducting this study.

Conflict of Interest

The authors have no conflicts of interest to declare.